

0017-9310(94)00332-7

# Local coefficients for forced convection in curved rectangular channels of large aspect ratio with unequal uniform heating

M. J. TARGETT,† W. B. RETALLICK‡ and S. W. CHURCHILL§

Department of Chemical Engineering, University of Pennsylvania, 311A Towne Building,  
 220 S. 33rd Street, Philadelphia, PA 19104-6393, U.S.A.

(Received 5 April 1994 and in final form 7 October 1994)

**Abstract**—A finite-element representation and the FIDAP™ code were used to solve the equations of conservation for mass, momentum and energy for fully developed angular flow and fully developed convection in the annulus between two concentric cylinders. Local Nusselt numbers were determined for a complete range of heat flux density ratios, both positive and negative, on the inner and outer surfaces, for Dean numbers up to  $2\frac{1}{2}$  times the critical value for the onset of vortical motion. The Nusselt numbers are found to depend strongly on the heat flux density ratio as well as on the Dean number. The applicability of the results to double-spiral heat exchangers is discussed.

## INTRODUCTION

The overall objective of the research, of which the work reported here is an essential element, is the prediction of the temperature and the concentration of contaminants in air flowing first inwardly and then outwardly through a double-spiral-catalytic incinerator with electric heating at the core, as shown schematically in Fig. 1. The catalyst is coated uniformly on the two thin corrugated metal plates out of which the device is constructed. The corrugations, which were intended to minimize planar distortions, are presumed to be too small in height to influence the flow significantly in the laminar regime, while the heat released on incineration is presumed to be too small to affect the energy balance significantly. The process itself is described in detail by Targett *et al.* [1]. Another proposed application of the double-spiral heat exchanger with reversing flow is for the combustion of low-heating-value fuels (those with insufficient heat of combustion to burn without significant preheating). The reason for the use of the double-spiral configuration in these and other related applications is the significant reduction of heat losses, as compared to conventional exchangers, by virtue of the minimal exposure of surfaces at high temperature to the surroundings.

The performance of double-spiral heat exchangers (particularly for large values of the number of transfer units  $N = UA/wc_p$ ) is characterized by a complex ther-

mal coupling between the inwardly flowing and outwardly flowing streams. During each turn of the channel through which the inwardly flowing stream passes (except for the most outward and the most inward ones), heat is not only received from the warmer out-

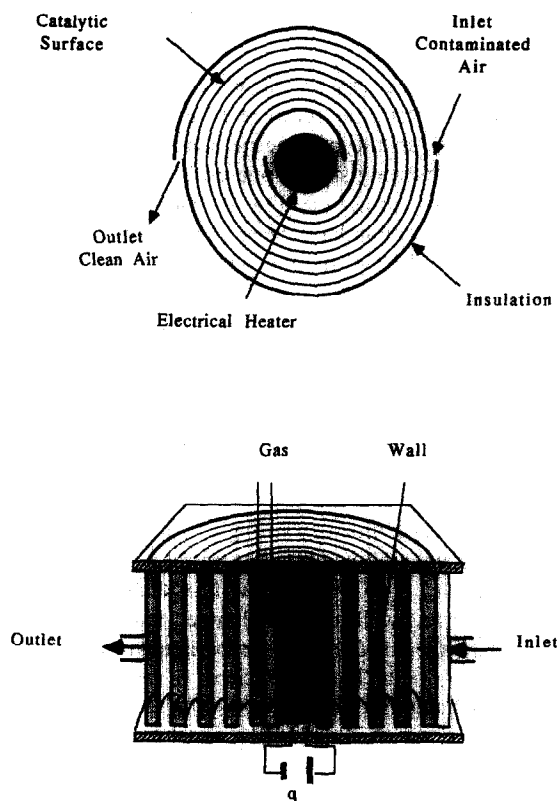


Fig. 1. Schematic diagrams of a four-turn double-spiral heat exchanger for incineration of contaminated air.

† Present address: E. I. DuPont Co., Wilmington, DE, 19880-0304, U.S.A.

‡ Address: W. B. Retallick Associates, 1432 Johnny's Way, West Chester, PA 19382, U.S.A.

§ Author to whom correspondence should be addressed.



an asymptotically small gap-to-radius-of-curvature ratio.

Experimental measurements of the rate of heat transfer in double spirals of rectangular cross section have been reviewed by Strenger *et al.* [3] who note that most of the results are for the turbulent regime and consist of overall mean coefficients for heat transfer for the entire exchanger based on the log-mean of the temperature differences at the inlet and exit. Strenger *et al.* did not themselves determine heat transfer coefficients, either local or overall, but their measurements of the temperature distribution along the internal surfaces of the exchanger reveal a nearly uniform temperature difference across the channels except for a turn or two near the periphery and a turn or two near the central core. This result is significant with respect to the work herein because it implies that the postulate of a locally uniform heat flux density on the surfaces can be used to simplify the differential energy balances.

**ASYMPTOTIC SOLUTIONS**

Solutions for the heat transfer coefficients for forced convection in flow between parallel plates can be considered to be asymptotes for angular flow through an annulus in the limit of vanishingly small gap-to-radius-of-curvature ratio. A solution for fully developed convection in fully developed laminar flow between uniformly but unequally heated parallel plates can be constructed (for example see ref. [7]) from the solution for one uniformly heated plate and one perfectly insulated plate by the principle of superposition. For heating of the 'inner' plate only, it can be shown that

$$T_i - T_m = \frac{13}{35} \left( \frac{j_i d}{k} \right) \tag{1}$$

while for heating of the 'outer' plate only

$$T_i - T_m = - \frac{9}{70} \left( \frac{j_o d}{k} \right). \tag{2}$$

Then for heating of both plates

$$T_i - T_m = \frac{13}{35} \left( \frac{j_i d}{k} \right) - \frac{9}{70} \left( \frac{j_o d}{k} \right) \tag{3}$$

which may also be expressed as

$$Nu_i \equiv \frac{j_i d}{k(T_i - T_m)} = \frac{35/13}{1 - \frac{9}{26} \left( \frac{j_o}{j_i} \right)}. \tag{4}$$

The corresponding expression for the outer plate is obviously

$$Nu_o \equiv \frac{j_o d}{k(T_o - T_m)} = \frac{35/13}{1 - \frac{9}{26} \left( \frac{j_i}{j_o} \right)}. \tag{5}$$

Equations (4) and (5) are valid for all values of  $j_i$

and  $j_o$ , both positive (for heating) and negative (for cooling). Equation (4) indicates that  $Nu_i$  is unbounded for  $j_o/j_i = \frac{26}{9}$  and negative for  $j_o/j_i > \frac{26}{9}$ , while equation (5) indicates that  $Nu_o$  is unbounded for  $j_o/j_i = \frac{9}{26}$  and negative for  $0 < j_o/j_i < \frac{9}{26}$ . These anomalies are not physical but merely an artifact of the arbitrary definitions of  $Nu_i$  and  $Nu_o$ . For example, the temperature on the 'inner' wall is simply equal to  $T_m$  for  $j_o/j_i = \frac{26}{9}$  and less than  $T_m$  for  $j_o/j_i > \frac{26}{9}$ . As will be shown below, equations (4) and (5) prove invaluable for interpreting and correlating the numerically computed values of  $Nu_i$  and  $Nu_o$  for curved channels.

The approximation for the effect of curvature devised by Langmuir [8] for external convection from a wire can be extended for internal convection from curved surfaces in the form

$$Nu_{ic} = \frac{d/r_i}{\ln \left\{ 1 + \frac{d}{r_i Nu_{ip}} \right\}} \cong Nu_{ip} + \frac{d}{2r_i} \tag{6}$$

and

$$Nu_{oc} = \frac{-d/r_o}{\ln \left\{ 1 - \frac{d}{r_o Nu_{op}} \right\}} \cong Nu_{op} - \frac{d}{2(r_i + d)} \tag{7}$$

where the subscripts c and p designate the Nusselt numbers for curved and straight channels, respectively. Equations (6) and (7) would be expected to be applicable only in the absence of secondary motion.

**NUMERICAL MODELING**

The segment of the channel to be modeled is shown schematically in Fig. 2 in order to define the variables.

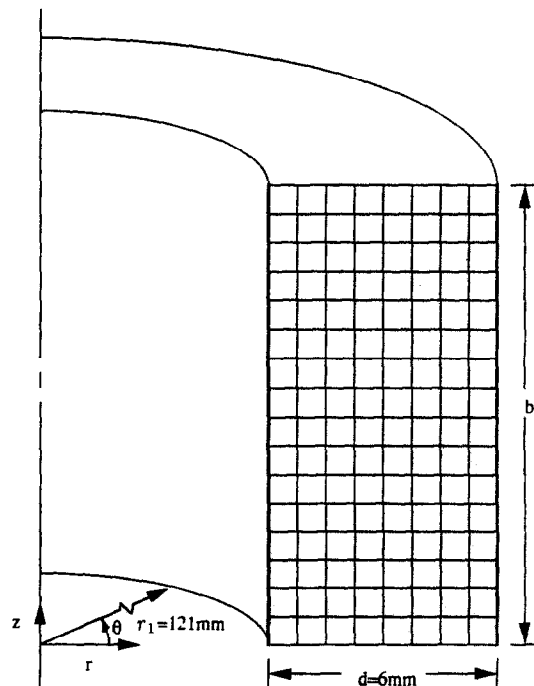


Fig. 2. Grid arrangement for finite-difference computation.

For a channel of infinite extent the distance  $b$  represents a trial value for the unknown wavelength  $\lambda$  of a pair of counter-rotating vortices. For a channel of finite aspect ratio the distance  $b$  corresponds to the half-breadth of the channel  $h/2$ .

The actual channel of interest consists of an Archimedean spiral (with a constant rate of change of radius with angle), but in the numerical modeling the effect of the changing radius is neglected, that is, at each distance through the coil the fields of velocity and temperature are postulated to be the same as in fully developed angular flow and fully developed convection, respectively, in the annulus between two concentric cylinders. This is the same idealization as that made by Baurmeister and Brauer [5] for a spiral coil of circular cross section, and is analogous to the idealization made by a number of investigators in neglecting the pitch of a helical coil.

The following additional postulates are made in the interests of simplicity:

- (1) invariant physical properties;
- (2) Newtonian behavior;
- (3) steady, axisymmetric, nonoscillatory flow;
- (4) negligible viscous dissipation.

The postulate of axisymmetry eliminates all derivations of the components of the velocity in  $\theta$ , but all three balances for momentum and all three components of the velocity must be retained to allow for a secondary motion. The equation for the conservation of mass can then be written in cylindrical polar coordinates as

$$\frac{1}{r} \frac{\partial}{\partial r} (ru_r) + \frac{\partial u_z}{\partial z} = 0 \quad (8)$$

the equations for the conservation of momentum as

$$\rho \left( u_r \frac{\partial u_r}{\partial r} - \frac{u_\theta^2}{r} + u_z \frac{\partial u_r}{\partial z} \right) = -\frac{\partial P}{\partial r} + \mu \left[ \frac{1}{r} \frac{\partial}{\partial r} \left( r \frac{\partial u_r}{\partial r} \right) + \frac{\partial^2 u_r}{\partial z^2} - \frac{u_r}{r^2} \right] \quad (9)$$

$$\rho \left( u_r \frac{\partial u_\theta}{\partial r} + \frac{u_r u_\theta}{r} + u_z \frac{\partial u_\theta}{\partial z} \right) = -\frac{1}{r} \frac{\partial P}{\partial \theta} + \mu \left[ \frac{1}{r} \frac{\partial}{\partial r} \left( r \frac{\partial u_\theta}{\partial r} \right) + \frac{\partial^2 u_\theta}{\partial z^2} - \frac{u_\theta}{r^2} \right] \quad (10)$$

$$\rho \left( u_r \frac{\partial u_z}{\partial r} + u_z \frac{\partial u_z}{\partial z} \right) = -\frac{\partial P}{\partial z} + \mu \left[ \frac{1}{r} \frac{\partial}{\partial r} \left( r \frac{\partial u_z}{\partial r} \right) + \frac{\partial^2 u_z}{\partial z^2} \right] \quad (11)$$

and the equation for the conservation of energy as

$$\rho c_p \left( u_r \frac{\partial T}{\partial r} + u_z \frac{\partial T}{\partial z} + \frac{u_\theta}{r} \frac{\partial T}{\partial \theta} \right) = k \left[ \frac{1}{r} \frac{\partial}{\partial r} \left( r \frac{\partial T}{\partial r} \right) + \frac{\partial^2 T}{\partial z^2} + \frac{1}{r^2} \frac{\partial^2 T}{\partial \theta^2} \right] \quad (12)$$

The criterion for fully developed convection with a uniform heat flux density  $j_i$  from the inner wall and a uniform heat flux density  $j_o$  from the outer wall can be expressed as

$$\frac{\partial}{\partial \theta} \left( \frac{k(T - T_m)}{j_i r_i + j_o r_o} \right) = 0 \quad (13)$$

from which it follows that

$$\frac{\partial T}{\partial \theta} = \frac{\partial T_m}{\partial \theta} \quad (14)$$

An overall energy balance for this condition can be expressed as

$$u_{\theta m} \rho c_p d \left( \frac{dT_m}{d\theta} \right) = j_i r_i + j_o r_o \quad (15)$$

From equations (14) and (15)

$$\frac{\partial^2 T}{\partial \theta^2} = \frac{\partial^2 T_m}{\partial \theta^2} = 0 \quad (16)$$

Substituting for  $\partial T/\partial \theta$  and  $\partial^2 T/\partial \theta^2$  in equation (12) from equations (14)–(16), and rearranging gives

$$u_r \frac{\partial T}{\partial r} + u_z \frac{\partial T}{\partial z} + \frac{u_\theta (j_i r_i + j_o r_o)}{r u_{\theta m} \rho c_p d} = \frac{k}{\rho c_p} \left[ \frac{1}{r} \frac{\partial}{\partial r} \left( r \frac{\partial T}{\partial r} \right) + \frac{\partial^2 T}{\partial z^2} \right] \quad (17)$$

The boundary conditions for a finite aspect ratio were chosen to be those for no slip and uniform heating at  $r = r_i$  and  $r = r_o$ , for symmetry at  $z = 0$ , and for no slip and no heat flux at  $z = h/2$ . An arbitrary temperature of  $T_i$  was specified at  $r = r_i$ . For an infinite aspect ratio the conditions at  $z = h/2$  were replaced by those for symmetry at  $z = b$ .

The chosen physical properties were  $c_p = 996 \text{ J kg} \cdot \text{K}^{-1}$ ,  $k = 0.0268 \text{ W} \cdot \text{m} \cdot \text{K}^{-1}$ ,  $\mu = 1.9 \times 10^{-5} \text{ Pa} \cdot \text{s}$ , and thereby  $Pr = 0.706$ . The chosen dimensions were  $r_i = 121 \text{ mm}$  and  $r_o = 127 \text{ mm}$ , thereby resulting in an annular gap  $d = 6 \text{ mm}$ .

The FIDAP† finite-element code that was used to solve these equations would not (logically enough) accept an angular pressure gradient for fully developed toroidal flow. Hence the angular pressure gradient was replaced by an equivalent body force, that is,  $-(\partial P/\partial \theta)$  in equation (10) was replaced by  $\rho G$ . Solutions for different pressure gradients were thereby generated by choosing a series of values of  $\rho$ . The value of  $G$ , which is arbitrary in this scheme, was chosen to be  $1 \times 10^{-3} \text{ m}^2 \cdot \text{s}^{-2}$ . As discussed below, the computational procedure differed somewhat for infinite and finite aspect ratios. The computations

† Trademark of Fluid Dynamics International, Inc.

were implemented at the Pittsburgh Supercomputing Center on a Cray Y-MP.

#### *Infinite aspect ratio*

The computations for an infinite aspect ratio were for a single wavelength since the velocity field is postulated to be periodic in this respect. This distance is not known in advance so computations for the velocity only were carried out for a series of axial distances  $b$ . The wavelength  $\lambda$  was then determined as the value of  $b$  for which the mean velocity in the angular direction is a minimum. The energy balance was solved only for this value of  $b$ .

The computational grid consisted of a  $17 \times 25$  mesh (in the  $r$  and  $z$  directions, respectively) with 425 modal points and 384 elements. The elements were four-noded, quadrilateral, and linear. The components of the velocity were approximated by bilinear interpolating functions and the pressure by a piecewise discontinuous approximation. The penalty-pressure method was used with  $\nabla \cdot \mathbf{v} = 1 \times 10^{-7}P$ . The strategy of solution consisted of 10 successive substitutive iterations followed by up to 500 quasi-Newton iterations. The tolerances for velocity-convergence and force-convergence were both set at 0.001. This tolerance was sufficient for close agreement with theoretical values for the critical Dean number and wavelength and with solutions in closed form for the velocity distribution and the friction factor for subcritical flow.

#### *Finite aspect ratios*

The computations for the velocity field for finite aspect ratios were more straightforward than those for an infinite aspect ratio in that the wavelength of the pairs of vortices did not need to be determined by trial and error. This gain was, however, at the expense of a greatly extended zone of computation. Since the ratio  $h/2d$  for each finite aspect ratio for which computations were carried out greatly exceeded  $\lambda/d$  for the infinite aspect ratio, a greater number of finite elements was necessary for the same degree of accuracy. In order to maintain approximately the same ratio of elements per vortex as for the infinite aspect ratio, grids of  $17 \times 45$ ,  $13 \times 72$ , and  $13 \times 88$  were used for aspect ratios of 5, 12, and 16, respectively. Except for the different boundary conditions as outlined above, the computational procedure was the same as for the infinite aspect ratio.

### COMPUTED CHARACTERISTICS

The field of velocity was computed for a series of specified values of the density in lieu of the pressure gradient (as explained above). The angular component of the computed velocity field was then integrated across the gap to determine the mixed-mean velocity, and in turn the Dean number

$$Dn \equiv \frac{du_{0m}\rho}{\mu} \left( \frac{d}{r_1} \right)^{1/2}$$

The arbitrary values of the density were chosen to yield values of  $Dn$  slightly below as well as somewhat above the critical value for the onset of stable vortical motion. Results for the velocity field and for the friction factor for both infinite and finite aspect ratios have previously been reported by Targett *et al.* [9]. The corresponding results for heat transfer for  $Pr = 0.706$  are presented here. The thermal calculations were first carried out for a wide range of conditions for an infinite aspect ratio, and then for a limited range of conditions for three large aspect ratios in order to determine the dependence on that parameter.

#### *Infinite aspect ratio*

For an infinite aspect ratio (corresponding to concentric cylinders of unbounded axial length) and Dean numbers less than a critical value, the field of flow as given by the analytical solution as well as by the numerical solution of Targett *et al.* [9] is purely angular but slightly distorted relative to that for flow between parallel plates. For rates of flow greater than that corresponding to the critical Dean number, a secondary motion in the form of a series of identical pairs of counter-rotating vortices was found to occur. As noted above, the wavelength of these vortices, which depends on the Dean number, is not known *a priori*. The wavelength was, however, determined by trial and error as the value that results in a minimum in the mixed-mean velocity and hence in the Dean number for a specified density (pressure gradient). The critical Dean number for an infinite aspect ratio and the chosen ratio of  $r_1/d = 20.17$  was determined by Targett *et al.* [9] to be 37.21, which is consistent with prior values determined by stability analyses.

In the current work the energy balance [equation (17)] was solved only for the Dean numbers and wavelengths corresponding to the minimum mixed-mean velocity for each specified density. The primary set of thermal computations was for uniform heating on only one of the two surfaces. The complete two-dimensional temperature field in the fluid was computed in each case but herein are reported only those dimensionless characteristic values that define the heat transfer coefficients. These characteristic values are listed in Table 1. It should be noted that  $T_i$ ,  $T_o$ , and  $T_m$  vary slightly and periodically with axial distance. The values reported here were averaged over a half a wavelength. The listed values of  $Nu_i^*$  and  $Nu_o^*$  are based on these averaged values of  $T_i$ ,  $T_o$ , and  $T_m$ .

The computed values of  $Nu_i^* = 2.731$  for subcritical heat transfer from the inner wall due to an imposed heat flux on that wall only may be observed in Table 1 to be independent of  $Dn$  and slightly greater than the value of  $Nu_i^* = \frac{35}{13} = 2.692$  given by equation (4) for flow between parallel plates, while the values of  $Nu_o^* = 2.647$  for heat transfer from the outer wall due to an imposed heat flux on that wall only are observed to be slightly smaller than the same value of 2.692

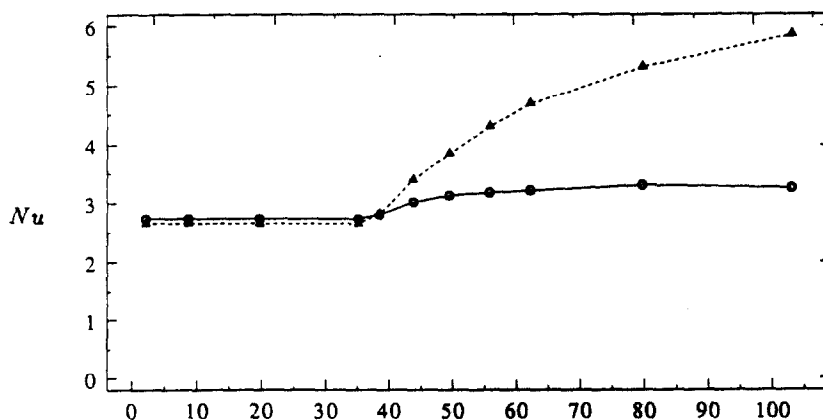
Table 1. Computed characteristics for fully developed convection in fully developed angular flow in the annulus between concentric circular cylinders of infinite length and  $r_1/d = 20.17$  with uniform heating on one wall

$Dn$	$\frac{\lambda}{d}$	$Nu_i^i$	$\alpha = \frac{(T_m - T_i)^o}{(T_i - T_m)^i}$	$Nu_o^o$	$\beta = \frac{(T_m - T_o)^i}{(T_o - T_m)^o}$
2.230	—	2.731	(0.3461)	2.647	(0.3461)
8.917	—	2.731	—	2.647	—
20.06	—	2.731	—	2.647	—
35.67	—	2.731	—	2.647	—
38.79	1.69	2.799	0.3320	2.809	0.3233
41.54	1.53	2.921	—	3.112	—
44.32	1.46	3.011	—	3.397	—
47.26	1.39	3.087	0.2247	3.642	0.2990
50.28	1.31	3.136	—	3.852	—
53.33	1.21	3.154	—	4.020	—
56.47	1.15	3.181	0.1960	4.204	0.2990
59.70	1.09	3.195	—	4.381	—
63.03	1.05	3.218	—	4.529	—
66.43	1.01	3.234	0.1826	4.683	0.2990
80.72	0.90	3.303	—	5.285	—
103.96	0.725	3.260	0.1733	5.856	0.2990

given by equation (5). The values given by the approximation of Langmuir [equation (6) combined with equation (4), and equation (7) combined with equation (5)] are  $Nu_i^i = 2.717$  and  $Nu_o^o = 2.668$ . The corrections provided by this approximation are in the right direction but insufficient numerically, presumably because of their failure to account for the distortion of the subcritical velocity profile. In any event the differences are very small and substantiate rather than denigrate the accuracy of the computations. The average of the computed values of  $Nu_o^o$  and  $Nu_i^i$ , namely  $(2.647 + 2.731)/2 = 2.689$  is slightly less than the value of 2.692 for parallel plates, although a slightly greater value would be anticipated,

again because of the distortion of the subcritical velocity profile by the curvature. This discrepancy undoubtedly reflects some error in the finite-element computations, but is in any event completely negligible for all practical purposes.

The computed values of  $Nu_i^i$  and  $Nu_o^o$  increase with  $Dn$  above its critical value, that is, after the onset of vortical motion. The dependence of  $Nu_i^i$  and  $Nu_o^o$  on  $Dn$  is shown graphically in Fig. 3.  $Nu_i^i$  increases only slightly and appears to attain a maximum value about 25% greater than the value of 2.731 for subcritical flow. On the other hand, the values of  $Nu_o^o$  rapidly exceed those for  $Nu_i^i$ , and continue to increase over the range of  $Dn$  encompassed by the computations,



$$Dn = \frac{d u_m \rho}{\mu} \left( \frac{d}{r_1} \right)^{1/2}$$

Fig. 3. Dependence of the computed values of  $Nu_i^i$  and  $Nu_o^o$  for an infinite aspect ratio on the Dean number. (Inner-radius-to-gap-ratio of 20.17.) (—○—)  $Nu_i^i$ ; (---△---)  $Nu_o^o$ .

attaining at  $Dn = 100$  a value about 2.25 times the value of 2.647 for subcritical flow.

The principle of superposition in terms of  $T - T_m$  might be expected to remain applicable for the regime of secondary motion owing to the linearity in terms of temperature of the energy balance [equation (17)] and the boundary conditions. On this basis, equation (4) can be generalized as

$$Nu_i = \frac{j_i d/k}{(T_i - T_m)^i + (T_i - T_m)^o} = \frac{Nu_i^i}{1 + \frac{(T_i - T_m)^o}{(T_i - T_m)^i}} = \frac{Nu_i^i}{1 - \alpha \left(\frac{j_o}{j_i}\right)} \quad (18)$$

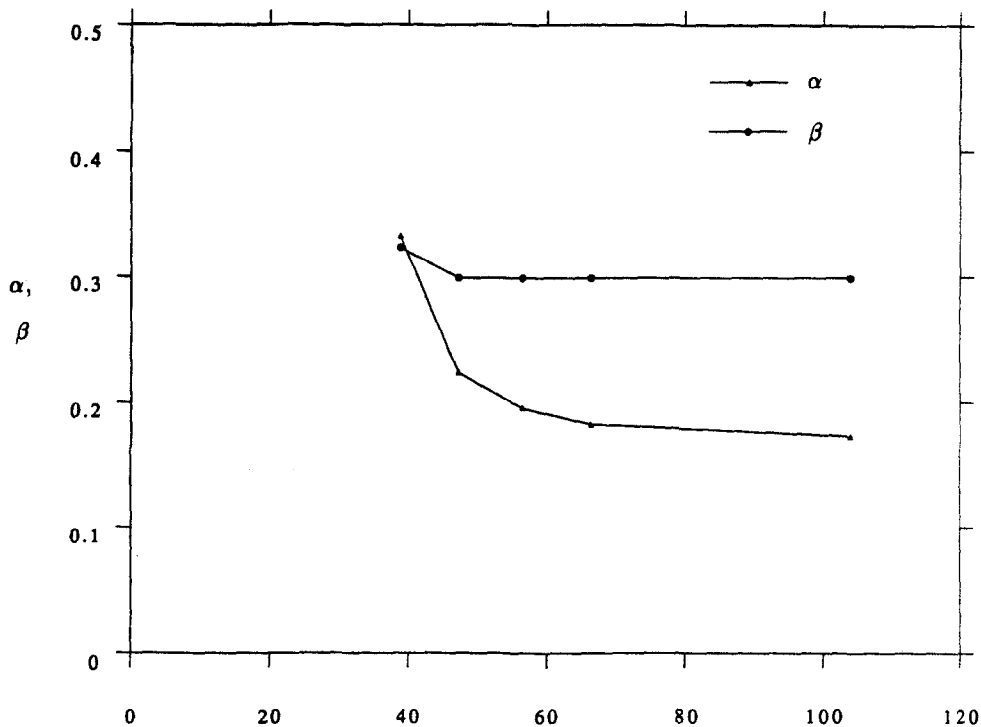
where  $(T_i - T_m)^i$  and  $(T_i - T_m)^o$  represent the contributions to  $T_i - T_m$  due to heating on the inner wall and heating on the outer wall, respectively. The computed values of the ratio  $(T_m - T_i)^o / (T_i - T_m)^i$  that are listed in Table 1 for representative values for  $Dn$  actually correspond to  $\alpha$  since the separate rates of heating in these computations were the same. The corresponding expression for the outer wall is

$$Nu_o = \frac{j_o d/k}{(T_o - T_m)^o + (T_o - T_m)^i} = \frac{Nu_o^o}{1 + \frac{(T_o - T_m)^i}{(T_o - T_m)^o}} = \frac{Nu_o^o}{1 - \beta \frac{j_i}{j_o}} \quad (19)$$

The computed values of  $(T_m - T_o)^i / (T_o - T_m)^o = \beta$  are included in Table 1 for the same values of  $Dn$ .

The computed values of both  $\alpha$  and  $\beta$  are plotted vs  $Dn$  in Fig. 4.  $Nu_i$  and  $Nu_o$  can be predicted for any value of the ratio  $j_o/j_i$ , positive or negative, and any value of  $Dn < 100$  using equations (18) and (19) and the values of  $Nu_i^i$ ,  $Nu_o^o$ ,  $\alpha$ , and  $\beta$  plotted in Figs. 3 and 4.

A set of computations was carried out for a complete range of values of  $j_o/j_i$  for  $Dn = 38.79$  (which is just above the critical value of 37.21) in order to test the following: (1) the applicability of the principle of superposition for this process; (2) the applicability of the differential model, the finite-element representation, and the computational algorithm for finite values of uniform but unequal rates of heating; and (3) the accuracy of the predictions of equations (18) and (19) using the values in Table 1 for  $Nu_i^i$ ,  $Nu_o^o$ ,  $\alpha$ ,



$$Dn = \frac{du_{\theta m} \rho}{\mu} \left(\frac{d}{r_1}\right)^{1/2}$$

Fig. 4. Dependence of the coefficients of equations (18) and (19) for an infinite aspect ratio on the Dean number. (Inner-radius-to-gap-ratio of 20.17.)

Table 2. Comparison of predictions of equations (18) and (19) with computed values for  $Dn \cong 39$ 

$j_o/j_i$	$Nu_i$		$Nu_o$	
	Computed	Equation (18)	Computed	Equation (19)
$-\infty$	0	0	2.799	2.799
-10.00	0.6474	0.6475	2.711	2.711
-4.00	1.201	1.201	2.590	2.590
-2.00	1.681	1.681	2.409	2.409
-1.25	1.976	1.977	2.224	2.224
-1.00	2.100	2.100	2.115	2.115
-0.80	2.209	2.210	1.993	1.993
-0.50	2.398	2.399	1.700	1.700
-0.25	2.582	2.583	1.221	1.220
-0.10	2.706	2.707	0.6611	0.6611
0	2.797	2.797	0	0
0.10	2.893	2.893	-1.250	-1.253
0.25	3.050	3.050	-9.539	-9.536
0.50	3.353	3.354	7.923	7.924
0.80	3.808	3.809	4.699	4.698
1.00	4.185	4.187	4.137	4.137
1.25	4.777	4.781	3.776	3.776
2.00	8.317	8.324	3.339	3.339
4.00	-8.538	-8.527	3.046	3.045
10.00	-1.206	-1.206	2.893	2.892
$\infty$	0	0	2.799	2.799

and  $\beta$  for  $Dn = 38.79$ . The results are summarized in Table 2. The agreement is excellent, providing confirmation in all three respects; the slight discrepancies are of the order of the expected numerical error in the computed values and therefore acceptable. On the other hand, the numerical behavior of the values of  $Nu_i$  and  $Nu_o$  in Table 2 would be quite bewildering in the absence of equations (18) and (19). This behavior is somewhat easier to interpret in Fig. 5 in which  $Nu_i$  and  $Nu_o$  are plotted vs  $j_o/j_i$ . As mentioned in connection with the solutions for parallel plates, the singularity in  $Nu_i^i$  at  $j_o/j_i = \alpha$  and in  $Nu_o^o$  at  $j_i/j_o = \beta$ , as well as the negative values, are simply artifacts of

their definition rather than physical anomalies. The strong variation in  $Nu_i$  and  $Nu_o$  with  $j_o/j_i$  is of practical importance because applications typically encompass the regions of near-singularity. The dimensionless temperatures on the walls are better behaved than the corresponding Nusselt numbers, but the latter are more convenient in applications (as illustrated subsequently), despite their erratic variation with  $j_o/j_i$ .

#### Finite aspect ratio

The velocity field was also computed by Targett *et al.* [9] for aspect ratios of 5, 12, and 16 at Dean numbers slightly above and slightly below the critical value for that geometry. In the computations for the finite aspect ratios, it was unnecessary to specify a wavelength, but the computational network had to be extended to encompass half of the axial length of the channel. (The associated computational demands are presumably responsible for the absence of prior computations for either flow or heat transfer at large aspect ratios. The use of a supercomputer was truly necessary for this phase of the work.)

The velocity field, even for very large aspect ratios, differs surprisingly from that for an infinite aspect ratio. For all rates of flow below that corresponding to the critical Dean number for the onset of vortices, Targett *et al.* [9] observed a slow boundary-layer-type of secondary motion around the entire periphery superimposed on the angular flow. Above the critical Dean number, which was found to differ only slightly from that for the unbounded region, vortical cells appeared but of unequal size. In particular the cell adjacent to each end was observed to be greatly extended in the axial direction.

The thermal results reported herein for finite aspect ratios are limited to a uniform heat flux density on only the outer wall and to  $Dn \cong 39$ . The resulting values of  $Nu_o^o$  were found to be 3.25 for  $h/d = 5$ , 2.83 for  $h/d = 12$ , and 2.78 for  $h/d = 16$ , as compared to

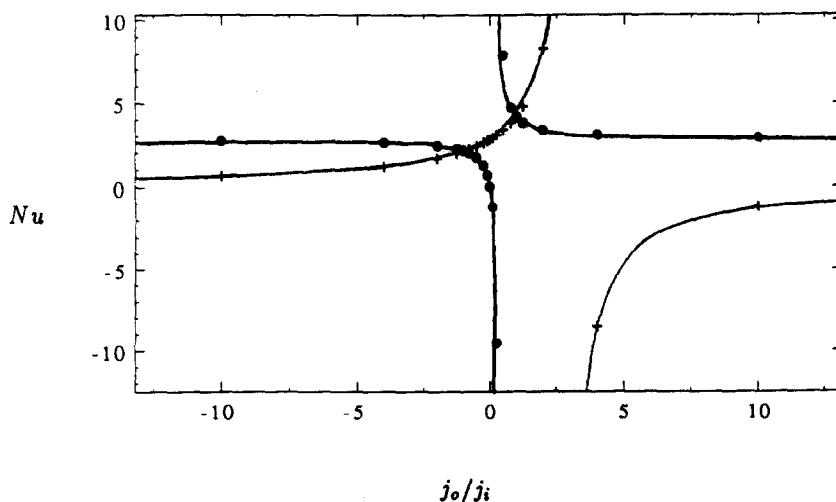


Fig. 5. Dependence of the Nusselt numbers for an infinite aspect ratio and  $Dn \cong 39$  on the heat flux density on the opposing walls. (Inner-radius-to-gap ratio of 20.17.) (+)  $Nu_i^i$ ; (●)  $Nu_o^o$ .

2.799 for  $h/d \rightarrow \infty$ . The slightly higher computed value for  $Nu_o^*$  for  $h/d = 16$  as compared to that for  $h/d \rightarrow \infty$  undoubtedly reflects computational error as well as slightly different values of  $Dn$  and is hardly surprising considering the different methods of computation that were employed. As indicated by the plot of these several values in Fig. 6, the value of  $Nu_o^*$  for an infinite aspect ratio appears to provide an adequate approximation for any aspect ratio greater than 10. This generalization can be inferred to hold for  $Nu_i^*$ ,  $Nu_o$ , and  $Nu_i$ , as well as for higher and lower Dean numbers.

#### APPLICATION OF THE COMPUTED VALUES TO DOUBLE-SPIRAL HEAT EXCHANGERS

The computed values presented herein are all for fully developed angular flow and fully developed convection in the annulus between two concentric cylinders (a torus of rectangular cross section) with an inner-radius-to-gap ratio of 20.17, a uniform heat flux density on one or both surfaces, invariant physical properties, and  $Pr = 0.706$ . These idealizations and restrictions should be recognized when applying the results as an approximation for real double-spiral heat exchangers.

First, a region of development of flow and of convection occurs near the entrances of most heat exchangers. In spirals of many turns the perturbation associated with an entrance would be expected to be negligible in an overall sense just as in conventional countercurrent exchangers of large length-to-diameter ratio.

On the other hand, the velocity field in a spiral channel continues to develop even beyond the entrance owing to the continually changing radius of curvature, and must thereby differ somewhat from the fully developed field of velocity in an annulus even at the same radius-to-gap ratio and Dean number. Fortunately, differences in the velocity field are known to result in lesser differences in the Nusselt number. This latter premise is supported by the small differences in  $Nu_o^*$  observed in Fig. 6, despite the great differences in the fields of velocity.

The Nusselt numbers computed herein are implied to be a function of  $Dn$  only and not separately of  $Re$  and  $d/r_1$ . Cheng *et al.* [10] concluded from their finite-difference solutions that the friction factor in curved channels of square cross section was not a separate function of  $r_1/d$  for values of  $r_1/d$  greater than 10. That conclusion may be presumed to hold, at least to a first approximation, for larger aspect ratios and for the Nusselt numbers. Further support in this regard is provided by Walowit *et al.* [11], who found from a stability analysis for a curved channel of infinite aspect ratio that the critical Dean number and the associated wavelength changed only slightly as  $r_1/d$  decreased even to 4.0.

The idealized solutions for the performance of double-spiral heat exchangers of Targett *et al.* [2], Stren-

ger *et al.* [3], and Chowdhury *et al.* [4] that postulate a uniform overall heat transfer coefficient for the entire exchanger, as well as the experimental measurements of the temperature distribution on the walls by Stenger *et al.*, suggest instead that the heat flux density on both the inner and outer surfaces is actually almost uniform except for the innermost and outermost turn or two. Hence the error arising from the postulate of locally uniform heat flux densities in the solutions derived herein is surely tolerable. [The postulates of fully developed convection and uniform heat flux densities are incorporated in the solutions by virtue of equation (14).]

The dependence on the Prandtl number was not investigated in this work. The finite-difference solutions of Cheng and Akiyama for the Nusselt number for uniformly heated, curved channels of square cross section suggest a proportionality to  $Pr^{1/4}$  for Dean numbers at the upper limit of the current work.

Finally, the effect of the variation of the physical properties through the exchanger can, as described below, be accounted for with small error by using the values at the local temperature and pressure. Also, owing to the small wall-to-wall spacings typical of double-spiral exchangers, the temperature difference and hence the property variations across a channel can be expected to be small and therefore approximated adequately by any sort of average.

Illustrative calculations for the performance of a double-spiral heat exchanger that take into account locally the values of the Nusselt numbers derived herein will not be presented here because of the critical dependence of the behavior on the many parametric choices, for example, the number of turns, the diameter of the core, and the angular locations of the entrances and exits. Such calculations are, however, fairly straightforward. One possible procedure is first to carry out the calculations for fixed values of  $Nu_o$  and  $Nu_i$ . The heat flux density ratios are then determined for each location, and the local heat transfer coefficients modified accordingly. At the same time, the local heat transfer coefficients are corrected for the local Dean number and the local temperature-dependent properties. That process is then repeated iteratively to convergence. Such an iteration was tested and found to be feasible.

Although the work reported herein was motivated by applications involving equal countercurrent rates of flow of the same fluid, the computed values of  $Nu_o$  and  $Nu_i$  are directly applicable for unequal rates of flow.

#### CONCLUDING REMARKS

This paper presents the first values for the local Nusselt numbers for angular flow in the annulus between two concentric circular cylinders (a torus of rectangular cross section). These results were obtained by solving the equations for the conservation of mass, momentum, and energy for steady state, fully

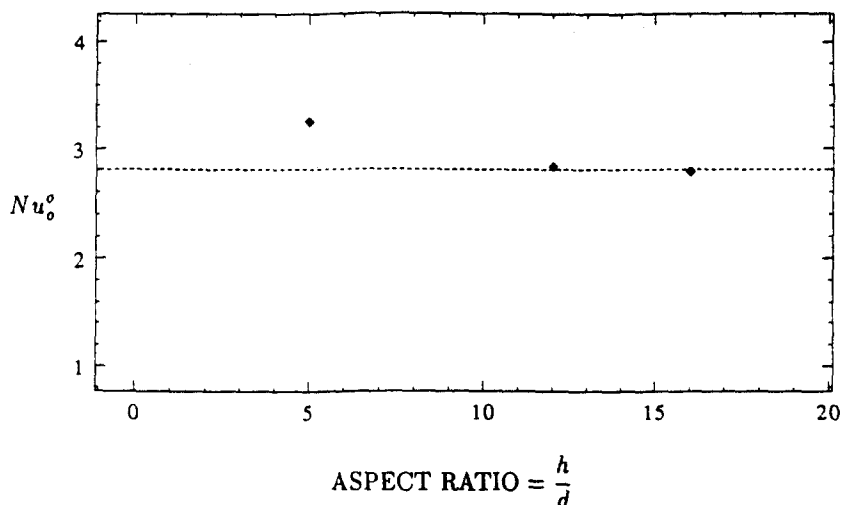


Fig. 6. Dependence of  $Nu_o$  on the aspect ratio for  $Dn \cong 39$ . (Inner-radius-to-gap ratio of 20.17.) ( $\blacklozenge$ ) Finite aspect ratio; (---) in finite aspect ratio.

developed flow and fully developed convection in a 0.706-Prandtl-number fluid with unequal, uniform heating on the walls and an inner-radius-to-gap ratio of 20.17.

The method of solution utilized a finite-element representation and the FIDAP<sup>TM</sup> code. The use of a supercomputer was necessary in order to attain convergent solutions for large finite aspect ratios.

The computed results for the field of velocity, which provide the basis for the computations for heat transfer, were shown in an earlier paper [9] to be in accord with prior results for limiting conditions.

The primary results obtained in this investigation consist of Nusselt numbers for heating on only one or the other of the walls in channels of infinite aspect ratio. These results extend from the regime of subcritical flow up to  $2\frac{1}{2}$  times the Dean number for the onset of vortical motion. The results for subcritical flow are in accord with solutions in closed form for fully developed convection in fully developed flow between parallel plates.

On the basis of the principle of superposition the results for heating on only one surface can be utilized to construct solutions for all heat flux density ratios, both positive and negative. A positive ratio results from either heating on both walls or cooling on both walls. A negative ratio results from heating on one wall and cooling on the other. The applicability of the premise of superposition for this process was tested and confirmed by supplementary computations.

Supplementary computations were also carried out for aspect ratios of 5, 12, and 16 to determine the value below which this parameter must be considered. Despite a great difference in the computed fields of flow, the Nusselt number for heating on the outer wall at a Dean number slightly above the critical value was found to change negligibly for aspect ratios greater than 10. This generalization is expected to be valid for

other heat flux density ratios and for both higher and lower Dean numbers.

On the basis of prior solutions for the critical Dean number for an infinite aspect ratio, the computed Nusselt numbers for an inner-radius-to-gap ratio of 20.17 are presumed to be a function only of the Dean number for inner-radius-to-gap ratios as low as 4.0.

The computed results are concluded to be applicable, within the restriction on the inner-radius-to-gap ratio mentioned in the previous paragraph, as a good approximation for true double-spiral heat exchangers in terms of the local Dean number.

*Acknowledgments*—The support of the National Science Foundation for the experimental work through SBIR grants ISI 8560638 and ISI 8619609 and for the computations through grant MSM 900037P at the Pittsburgh Supercomputing Center is gratefully acknowledged.

## REFERENCES

1. M. J. Targett, S. W. Churchill and W. B. Retallick, The incineration of contaminants in air with a double-spiral heat exchanger-catalytic reactor, *Proc. Fourth World Congress of Chemical Engineering*, pp. 842–849, Karlsruhe (1991).
2. M. J. Targett, W. B. Retallick and S. W. Churchill, Solutions in closed form for a double-spiral heat exchanger, *Indust. Engng Chem. Res.* **31**, 658–669 (1992).
3. M. R. Strenger, S. W. Churchill and W. B. Retallick, Operational characteristics of a double-spiral heat exchanger for the catalytic incineration of contaminated air, *Indust. Engng Chem. Res.* **29**, 1977–1984 (1990).
4. K. Chowdhury, H. Linkmeyer, M. K. Bassiouny and H. Martin, Analytical studies on the temperature distribution in spiral plate heat exchangers: straightforward design formulae for efficiency and mean temperature difference, *Chem. Engng Process.* **19**, 183–190 (1985).
5. U. Baummeister and H. Brauer, Laminare Strömung und

- Wärmeübergang in Rohrwendeln und Rohrspiralen, *V.D.I. Forschung*, **593**, 1–48 (1979).
6. K. C. Cheng and M. Akiyama, Laminar forced convection heat transfer in curved rectangular channels, *Int. J. Heat Mass Transfer* **13**, 471–490 (1970).
  7. S. W. Churchill, *Laminar Forced Convection in Channels*. Book in preparation.
  8. I. Langmuir, Convection and conduction of heat in gases, *Phys. Rev.* **34**, 401–422 (1912).
  9. M. J. Targett, W. B. Retallick and S. W. Churchill, Flow through curved rectangular channels of large aspect ratio, *AIChE J*, in press.
  10. K. C. Cheng, R.-C. Lin and J.-W. Ou, Fully developed channel flow in curved rectangular channels, *J. Fluids Engng Trans. ASME* **98**, 41–48 (1976).
  11. J. Walowit, S. Tsao and R. C. Di Prima, Stability of flow between arbitrarily spaced concentric cylindrical surfaces including the effect of a radial temperature gradient, *J. Appl. Mech.* **31**, 585–593 (1964).